Eur. Phys. J. D **12**, 181–184 (2000)

THE EUROPEAN PHYSICAL JOURNAL D

EDP Sciences

Continuum light emission from sputtered species of graphite during ion beam irradiation

A. Qayyum[a] and M.N. Akhtar

Accelerator Laboratory, NPD, PINSTECH, P.O. Nilore, Islamabad, Pakistan

Received 24 September 1999 and Received in final form 11 February 2000

Abstract. Light emission during sputtering of graphite targets with 1–10 keV Ne^+, Kr^+ and Xe^+ beams has been investigated in the 180–600 nm wavelength range. Beside the characteristic lines of sputtered C_1 and C_1^+, a continuum superimposed with a number of broad structures was observed in the 250–520 nm range, and having a maximum at 386 nm. Mass analysis of the sputtered flux confirmed the presence of negative carbon clusters C_m^- ($m \leq 4$), C_2^- being the dominant one. Ion beam parameters *i.e.* ion mass, energy, current density and ion dose were varied to identify the origin of the continuum emission. On the basis of the experimental results, it is suggested that the continuum is predominantly due to the overlapping of various band systems of sputtered C_2 with a small contribution from the heavier sputtered carbon clusters C_m ($m > 2$).

PACS. 34.50.Dy Interactions of atoms, molecules, and their ions with surfaces; photon and electron emission; neutralization of ions – 36.40.-c Atomic and molecular clusters – 79.20.-m Impact phenomena (including electron spectra and sputtering)

1 Introduction

During energetic ion surface collisions, many secondary processes occur such as reflection of the projectile, electron ejection and sputtering of atomic, molecular and cluster species. Optical spectra of the sputtered flux mostly consist of lines from the sputtered neutrals and ions [1]. However, beside these discrete lines, broad band continuum emission is also observed to be the dominating feature in some cases. During sputtering at least four sources of continuum radiation have been identified:

1. emission from sputtered excited clusters and molecules, that are created as a result of collision processes occurring in the near surface region [2]. Continuum light from excited clusters and molecules have been observed up to few cm from the surface because of their comparatively longer radiative decay lifetimes (10^{-7}–10^{-5} s),
2. radiative recombination of electrons with trapped holes are responsible for band emission during irradiation of insulators with ion beams [3]. Thus emission is strictly a solid state phenomenon taking place at the target surface,
3. emission from the release of already implanted atoms. These particles are released as excited molecules during sputtering and de-excite in front of the surface. Molecular Ar [4] and Xe [5,6] have been reported in the sputtered flux,
4. some of the continuum radiation from metal surfaces is believed to be the result of radiative relaxation of collective oscillations of the free electrons (plasmons) [7,8].

In ion surface collisions it is of great interest to understand how sputtered molecular and cluster species are formed, excited and ionized. Much work is needed to understand the state of sputtered molecular and cluster species, their radiative decay lifetime, their de-excitation and their neutralization characteristics. In this work, we have performed simultaneous light and mass analysis of carbon flux sputtered from graphite targets bombarded with 1–10 keV inert gas ions. An extraordinary broad band emission from sputtered species of graphite was observed in the 250–520 nm wavelength range. The mechanism of its formation and variation of its shape and intensity with the ion beam parameters are investigated and the origin of the continuum emission is discussed.

2 Experimental setup

The experimental setup has been previously described in detail [9] and only a brief description is given here. The setup was developed purposefully for simultaneous light and mass analysis of sputtered flux. Ions were produced in a magnetically confined hollow cathode duoplasmatron [10] and their energy could be varied from 1 to 20 keV. The current density at the target surface was in the 20–200 μA/cm^2 range. The vacuum in the target chamber was

[a] e-mail: qayyum.pins@dgcc.org.pk

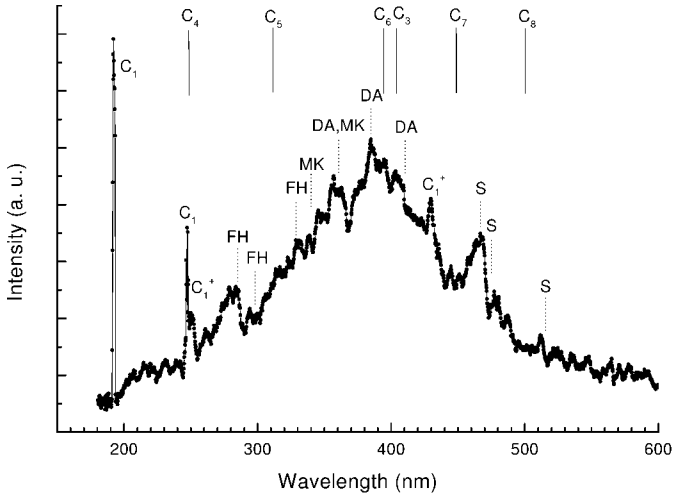

Fig. 1. The optical spectrum, in the 180–600 nm range, of the graphite bombarded with 10 keV Xe^+ beam, recorded with 0.2 nm spectral resolution and taken after irradiation of about 10^{18} Xe ions. Wavelength positions [12] of the known C_2 systems: Deslandres-D'Azambuja (DA), Fox-Herzberg (FH), Swan (S), Messerle-Kraussare (MK) are marked by vertical doted lines. The predicted positions [12,13] of C_m $(3 \leq m \leq 8)$ are indicated by vertical solid lines.

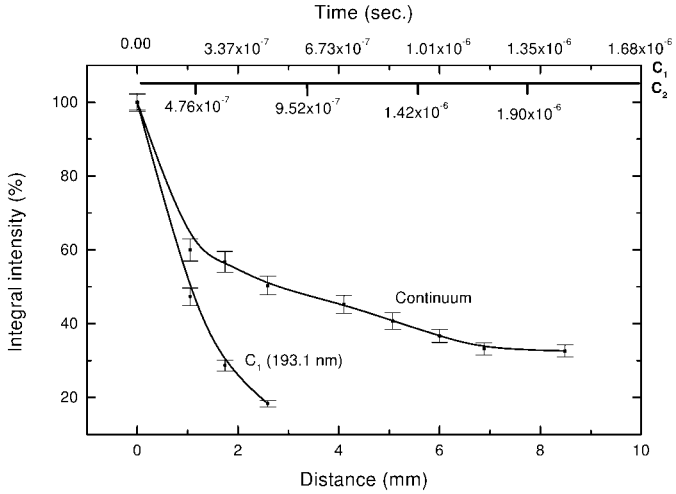

Fig. 2. Integral spatial intensity distribution for the continuum and the C_1 line (193.1 nm) emitted from the graphite target surface, bombarded by 10 keV Xe^+ beam. Figure 2 also shows the calculated excited lifetimes of C_1 and C_2 as a function of distance from the target, taking the energy of C_1 and C_2 equal to half of the surface binding energy [14] of graphite.

ensured by an ion pump down to 10^{-8} mbar and kept at 10^{-6} mbar throughout the experiment. For simultaneous light and mass analysis, both the light and the mass spectrometer were placed at the angle of 45° with respect to the incident beam. The spectral analyses were performed by a Jobin Yvon H20 monochromator in the 180–600 nm range through a fused silica window and the light was detected with the help of a photomultiplier tube. The grating of the monochromator was rotated by a stepper motor controlled by a computer through a GPIB interface. Mass analyses were carried out by a compact permanent magnet based velocity filter. The collimating apertures, placed in front of the velocity filter, restrict the divergence of the extracted beam to ±0.2°. Charged particle detection was done by a channel electron multiplier. The graphite target was mechanically polished and before each measurement it was sputter cleaned with 1 keV Xe^+ beam.

3 Results and discussion

Figure 1 shows a spectral scan taken with 10 keV Xe^+ beam over the 180–600 nm wavelength range. It has at least three very distinct features, namely sharp lines from C_1, C_1^+, a continuum which covers almost the entire spectrum (250–520 nm) with a maximum at 386 nm and a number of broad peaks superimposed particularly at 285.5, 299, 328.5, 360.7, 386, 410.2 and 468 nm. These peaks have been studied with 0.2 nm resolution and were found to have the width of several tens of nm. Thus these structures are bands of limited spectral extent. The sharp C_1 lines at 193.1 and 247.8 nm are coming from the transitions $3^1P_1^0 \rightarrow 2^1D_2$ and $3^1P_1^0 \rightarrow 2^1S_2$ respectively. Since this communication is about the continuum radiation the discrete lines will not be discussed here. However the identified lines are marked in Figure 1 and discussed elsewhere [9]. The emission lines and bands are interpreted using references [11–13]. It is hard to relate this broad emission with surface contamination because a decrease in its intensity was not noticed after prolonged target cleaning with Xe^+ beam. Also mass analysis of the sputtered flux did not confirm the presence of any surface contamination.

Next we established that broad emission was coming from the sputtered species and not confined to the surface. This conclusion has been drawn by placing the target at a position where the angle between the optical axis and the target surface normal was 100° [9]. At this angle the spectrometer cannot see the beam spot on the target and light was recorded only from those sputtered particles that were at least 3 mm away from the surface. We still recorded the continuum superimposed with broad structures but the carbon atomic lines (193.1, 247.8 nm) were missing. Figure 2 shows the spatial distribution of integral intensity of the C_1 (193.1 nm) line and the continuum radiation in front of the target surface. Since the energy $U_o/2$ of the sputtered particles, U_o being the surface binding energy [14], does not change significantly with mass, the expected lifetimes of sputtered excited C_1 and C_2 as a function of the distance from the target surface are shown in Figure 2. Most of the atomic emission from sputtered C_1 occurs within 1 mm from the surface, whereas the source of continuous radiation exists up to 10 mm from the surface. This clearly indicates that the source of continuum emission has molecular radiative decay lifetimes (10^{-7}–10^{-5} s).

We conducted a variety of tests to determine whether the continuum and the broad structures were in any way

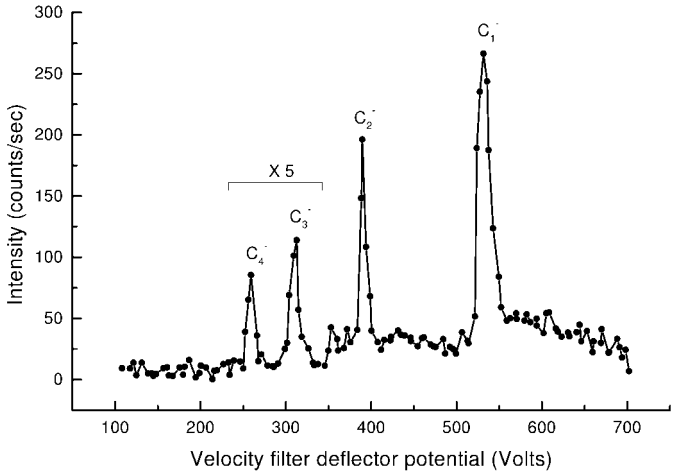

Fig. 3. A mass spectrum is shown identifying the peaks due to C_1^-, C_2^-, C_3^- and C_4^-; the latter two peaks are shown as multiplied by a factor of 5.

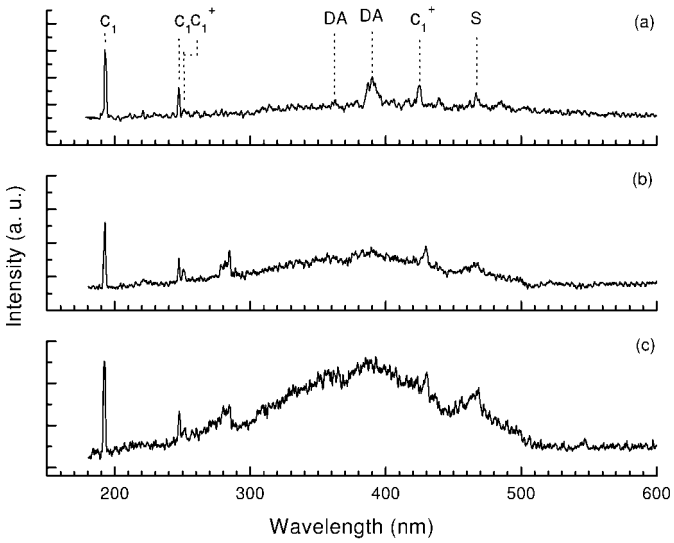

Fig. 4. Optical spectra of graphite bombarded with 10 keV Xe^+ taken after irradiations by (a) 10^{17}, (b) $5 \times 10^{17}$and (c) 2×10^{18} Xe^+ particles. (a–c) show how the continuum grows with the fluence while at the start of experiment (a) only the few heads of DA and S systems of C_2 along with atomic (193.1, 247.8 nm) and ionic (426.7, 251.2 nm) lines were recorded.

related to the incoming ion beam. Use of Ne^+, Kr^+ and Xe^+ beams produced exactly the same spectral distribution, but the intensity of the continuum showed slight rise with ion beam mass. Its intensity was not strongly dependent on the energy deposited during sputtering. However a linear relationship between the continuum intensity and the ion beam current density was observed for the 10 keV Xe^+ beam. The continuum emission cannot be related to the molecular emission of the implanted beam particles because the experiment was started with a heavy ion beam to avoid deep implantation and after every gas change the target was sputtered clean to remove the implanted beam atoms.

The unambiguous identification of carbon clusters comes from the mass analyses of the sputtered flux. Figure 3 shows the negative ion mass spectrum and corresponding peaks to be due to C_1^-, C_2^-, C_3^- and C_4^-. The C_2^- is the most dominant cluster in the sputtered flux while the intensity of C_3^- and C_4^- is about an order of magnitude lower. The heavier clusters C_m $(m > 4)$ may exist in the sputtered flux but their number is below the detection capability of our mass analyzer. In sputtering, the formation of "nascent" clusters take place essentially within the lifetime of the collision cascade developing in the solid (several hundred femtoseconds) and most of the clusters with $m = 3, 4$ and virtually all clusters with $m \geq 5$ are found to be unstable because of their high internal energies. Molecular dynamic computer simulations and theoretical analysis based on the Rice-Ramsberg-Kassel (RRK) theory indicate that due to fragmentation chains, involving many individual decomposition steps, these clusters are decomposed into stable fragments within few tens of picoseconds after their ejection [15] and at the end of decomposition process the dominating fragments are dimers and atoms [16]. On the time scale of the experiment, namely $\sim 10^{-8}$–10^{-5} s, only stable clusters can be detected [17]. The prominent superimposed structures, shown in Figure 1, are all due to various band systems of C_2. The Deslandres-D'Azambuja system (358.7, 360.7, 386, 410.2 nm) is the strongest observed one whereas other C_2 systems like the Fox-Herzberg (285.5, 299, 328.5 nm), the Swan (468, 473.7, 516.5 nm), and the Messerle-Krauss (339.6, 340.6, 358.6, 362.7, 367.3 nm) are also fairly strong. The radiative decay lifetimes of these band systems are in the 0.04−18 μs range [18], therefore, it is likely that both the sputtered as well as the decomposed C_2 contribute to these band emissions. We could not identify the emission bands of heavier carbon clusters but the predicted wavelength positions [12,13] of C_m $(3 \leq m \leq 8)$ also fall in the continuum region and they have been marked in Figure 1.

The most interesting observation is the growth of the continuum with ion beam fluence. As it can be seen in Figure 4, the continuum is almost missing at the start of an experiment and only the main heads of Deslandres-D'Azambuja and Swan systems of C_2 are prominent along with the C_1 and C_1^+ lines. It appears when the 10 keV Xe^+ beam fluence increases and saturates after an irradiation by 10^{18} particles. Formation of the continuum is due to the growth of other C_2 bands with the ion beam irradiation of the target. Mass analysis has confirmed an about three times increase in C_m^- $(2 \leq m \leq 4)$ intensity in the sputtered flux during this period. The increase of C_m^- $(2 \leq m \leq 4)$ sputtering yield with the ion beam irradiation of the graphite target may be due to the structures which develop on the target surface with the irradiation or deposition of the lose carbon soot on the target. During recently conducted experiments with a carbon cluster ion source [19,20] we have also noticed the increase of carbon cluster sputtering from the reconstituted cathode surface with the freshly adsorbed carbon layer-the regenerative soot. Nevertheless, the enhanced C_m^- $(2 \leq m \leq 4)$ sputtering yield points to a reduction in the binding force

of the surface constituents or a change of surface topography which supports carbon cluster sputtering.

The experimental results presented here suggest that the observed continuum emission during sputtering of graphite with 1–10 keV inert gas ions is predominantly due to the overlapping of various band systems of sputtered C_2 with small contributions from bands of heavier sputtered carbon clusters. Mass analysis showed that intensity of C_2 was an order of magnitude higher than C_3 and C_4 in the graphite's sputtered flux. However, the increase of carbon cluster sputtering with ion beam fluence cannot be explained on the basis of these results.

We greatly acknowledge the discussions with Dr. Shoaib Ahmad. Technical support of Ishfaq Mehmood, Sher Ahmad and Ali Akhter is appreciated.

References

1. A.R. Knudson, D.J. Nagel, J. Comas, K.W. Hill, Nucl. Instrum. Meth. **149**, 507 (1978).
2. C.W. White, N.H. Tolk, J. Kraus, W.F. van der Weg, Nucl. Instrum. Meth. **132**, 419 (1976).
3. N.H. Tolk, D.L. Simms, E.B. Foley, C.W. White, Radiat. Effects **18**, 221 (1973).
4. M. Braun, B. Emmoth, Nucl. Instrum. Meth. **170**, 585 (1980).
5. Th. Weber, K.P. Lieb, Nucl. Instrum. Meth. B **44**, 54 (1989).
6. R. Kuduk, J. Zuk, D. Maczka, Nucl. Instrum. Meth. B **85**, 794 (1994).
7. Yu.A. Bandurin, L.S. Belykh, I.E. Mitropolsky, A.I. Dashchenko, S.S. Pop, Nucl. Instrum. Meth. B **58**, 448 (1991).
8. Yu.A. Bandurin, A.I. Dashchenko, I.E. Mitropolsky, S.S. Pop, Nucl. Instrum. Meth. B **78**, 159 (1993).
9. A. Qayyum, M.N. Akhter, T. Riffat, S. Ahmad, Appl. Phys. Lett. **75**, 4100 (1999).
10. A. Qayyum, S. Ahmad, Nucl. Instrum. Meth. B **94**, 597 (1994).
11. *CRC Handbook of Chemistry and Physics*, 76th edn. (CRC Press Inc., New York, 1996), 10-13, 10-137.
12. R.W.B. Pease, A.G. Gaydon, *Identification of Molecular Spectra*, 4th edn. (Chapman and Hall, London, 1976), pp. 83-87.
13. W. Kratschmer, N. Sorg, D.R. Huffman, Surf. Sci. **156**, 814 (1985).
14. M.W. Thompson, Phys. Rep. **69**, 335 (1981).
15. A. Wucher, N.Kh. Dzhemilev, I.V. Veryovkin, S.V. Verkhoturov, Nucl. Instrum. Meth. B **149**, 285 (1999).
16. A. Wucher, Nucl. Instrum. Meth. B **83**, 79 (1993).
17. N.Kh. Dzhemilev, A.M. Goldenberg, I.V. Veriovkin, S.V. Verkhoturov, Nucl. Instrum. Meth. B **114**, 245 (1996).
18. W. Weltner Jr, R.J. van Zee, Chem. Rev. **89**, 1713 (1989).
19. S. Ahmad, T. Riffat, Nucl. Instrum. Meth. B **152**, 506 (1999).
20. S. Ahmad, Eur. Phys. J. AP **5**, 111 (1999).